

Growth and characterization of Sb₂Se₃ thin films for solar cells

T.M. Razykov*, A.X. Shukurov, O.K. Atabayev, K.M. Kuchkarov, B. Ergashev, A.A. Mavlonov

Physical-Technical Institute, Uzbekistan Academy of Science, Bodomzor Yo'li Str. 2B, 100084 Tashkent, Uzbekistan

ARTICLE INFO

Keywords:

Thin film
Sb₂Se₃
Absorber layer
Chemical molecular beam deposition

ABSTRACT

The growth of antimony selenide (Sb₂Se₃) thin films the first time by atmospheric pressure chemical molecular beam deposition (CMBD) method has been reported. The morphological and structural properties of the films were studied as a function of the hydrogen flow rate at different substrate temperature. Experimental data indicate that Sb₂Se₃ films grown as Se-rich at low hydrogen flow rate and the samples have almost amorphous structure. In contrast, at higher hydrogen flow rate, the films have Sb-rich composition and polycrystalline structure. Interestingly, transition from amorphous to polycrystalline structure is depend on the flow rate of the transport gas, while surface morphology affected by the substrate temperature. Electrical and optical measurements revealed that polycrystalline films have p-type conductivity and optical bandgap of 1.1 eV with high absorption coefficient of 10⁵ cm⁻¹. These results showed that the CMBD grown films can be used as absorber layer for fabrication of thin film solar cells.

1. Introduction

Power generation by using cost effective and ecologically friendly photovoltaic (PV) materials is one of the key factors for development of sustainable renewable energy sector (Polman et al., 2016). Currently, solar cells based on silicon (Si), CdTe and Cu(In,Ga)Se₂ have reached power conversion efficiency (PCE) of > 20% and became leading materials in the world PV market (Green et al., 2017; Jackson et al., 2016; Yoshikawa et al., 2017). However, high production cost of Si wafers, high price of Ga and In elements and toxicity issues of Cd are main limitations for PV power generation entering to multi-terawatt regime (Guha, 2017; Zakutayev, 2017). Hence, novel material systems consisting of non-toxic and earth-abundant elements have emerged. In the last decade, several compounds including metal sulphides and selenides such as Cu₂ZnSnSe₄ (Hartnauer et al., 2016), Cu₂SnS₃ (Chantana et al., 2017) CuSbS₂, (Whittles et al., 2017), SnSe (Razykov et al., 2018) and Sb₂Se₃ have been explored as an alternative and promising photovoltaic absorbers (Guha, 2017). Among them, antimony selenide (Sb₂Se₃) has emerged as a very suitable photovoltaic absorber material due to its excellent electro-optical properties (Sun et al., 2016). For example, Sb₂Se₃ has an optical bandgap of about 1.1 eV, high absorption coefficient (> 10⁵ cm⁻¹) and rather simple composition, i.e. compared to Cu(In,Ga)Se₂ thin film solar cells (Chen et al., 2015; Bajpeyee, 2012). Furthermore, research efforts on Sb₂Se₃ based thin film solar cells have already yielded with measurable conversion efficiency of above 7.5% over the past 3–4 years (Choi et al., 2014; Li et al., 2018; Tiwari et al.,

2018; Wen et al., 2018; Yuan et al., 2016). Since, the Sb₂Se₃ layer is the key material in Sb₂Se₃ based thin film solar cells, the crystalline quality of the film is crucial. In literature, Sb₂Se₃ thin films have been reported which were deposited using various growth methods, e.g. thermal evaporation (Liu et al., 2014), chemical bath deposition (Kulkarni et al., 2015), magnetron sputtering (Siol et al., 2016), spin-coating (Zhou et al., 2014), close-spaced sublimation (Wen et al., 2018), aerosol assisted chemical vapour deposition (AACVD) (Khan et al., 2018) etc. In this work, possible fabrication of Sb₂Se₃ thin films by chemical molecular beam deposition (CMBD) method has been reported.

2. Experimental

Polycrystalline Sb₂Se₃ precursor with the stoichiometric composition was used as source materials. The preparation of Sb₂Se₃ precursor as follows: Sb and Se granules (with high purity of 99.999%) was loaded into a closed quartz crucible, i.e. under vacuum. Subsequently, the quartz crucible was placed in the furnace to heat at 900 K for 8 h to synthesize Sb₂Se₃ compound. Finally, quartz crucible was rapidly cooled to room temperature (RT). The crystal structure of obtained Sb₂Se₃ precursor was found to be orthorhombic by X-ray diffraction (XRD) measurements.

The preparation of Sb₂Se₃ thin films was carried out in line with the procedure described in (Razykov, 1991). The Sb₂Se₃ precursor was loaded to the evaporator of the growth chamber and let the hydrogen flow for 10 min. in order to remove atmospheric pollutants from the

* Corresponding author.

E-mail address: razykov@uzsci.net (T.M. Razykov).

chamber. Afterwards, the outer furnace of the chamber was turned on. When the heating level of the substrate reached the required temperature, the individual heater was turned on in order to regulate the evaporator temperature. The temperature of evaporation was set to 900 K, i.e. slightly higher than the melting point of Sb_2Se_3 in order to avoid the low deposition rate depicted at evaporation temperature below 885 K, whereas higher evaporation temperatures (> 950 K) yielded Se-deficient films, which will be discussed elsewhere. The substrate temperature (T_s) was varied within the range of (670–790) K. The carrier gas, i.e. hydrogen, with different flow rates of (5–20) cm^3/min was used during the deposition process. The duration of the deposition process set to 30 min. All Sb_2Se_3 thin films were deposited on (20 × 20) mm^2 in size borosilicate glasses, which were cut into (10 × 10) mm^2 pieces using a diamond saw in order to investigate their structural, morphological, electrical and optical properties.

The crystal structure Sb_2Se_3 thin films were investigated by XRD measurements using a “Panalytical Empyrean” diffractometer (Cu K α radiation, $\lambda = 1.5418$ Å) with a wide-angle measurements of 2θ in the range of (10–90)° with a measurement steps of 0.01°. The experimental results were studied using the ‘Joint Committee on Powder Diffraction Standard’ (JCPDS, № 15-0861 for Sb_2Se_3). Morphological and chemical composition of the samples were investigated using a scanning electron microscope (SEM-EVO MA 10) and an energy-dispersive X-ray spectroscopy (EDX, Oxford Instrument - Aztec Energy Advanced X-act SDD) at an electron acceleration voltage of 15 kV, respectively. Optical bandgap of selected Sb_2Se_3 film was estimated from the transmission spectra obtained by spectrophotometer (HR4000, Ocean Optics). To perform electrical measurements, ohmic contacts were realized by vacuum deposition of silver on the films. The electrical conductivity of films were measured by van der Pauw method. The type of conductivity of the samples was determined by thermoelectric effect. The thickness of the films (1–2) μm was determined using micro-interferometer MII-4.

3. Results and discussion

Fig. 1 shows the wide-angle 2θ - ω scans for Sb_2Se_3 thin films grown in different flow rate of the hydrogen at fixed evaporation temperature of 900 K. JCPDS card of orthorhombic Sb_2Se_3 has been used for matching the diffracted peaks. In general, all samples had the high background of the XRD pattern, which was argued to come from the low incident angle (Ren et al., 2015). As shown, Sb_2Se_3 films grown in lower hydrogen flow rate of 5 and 7 cm^3/min at lower T_s of 670 K and

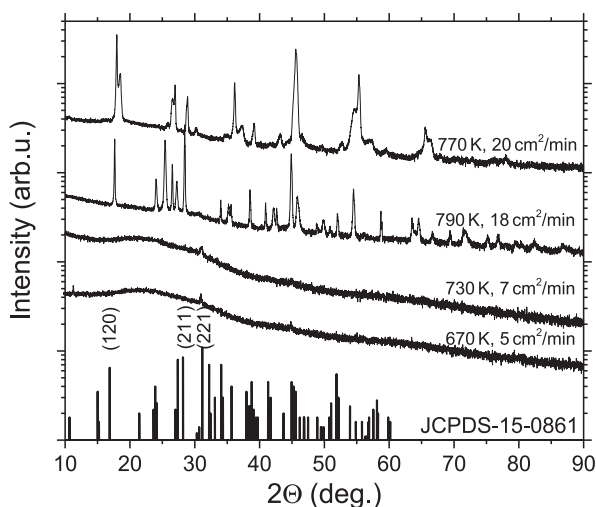


Fig. 1. Wide-angle X-ray diffraction data of Sb_2Se_3 films grown in different hydrogen flow rate at indicated substrate temperatures. Note that ‘Joint Committee on Powder Diffraction Standards’ (JCPDS) card of orthorhombic Sb_2Se_3 (15-0861) was used for the matching of the diffraction peaks.

730 K, have almost amorphous structure. Since, Sb_2Se_3 films grown by similar method of chemical vapour deposition had polycrystalline structure at $T_s = 670$ K (Razykov et al., 2017), this amorphous structure of the films may be caused by the low flow rate of the carrier gas. This is also evident from literature that amorphous structure of Sb_2Se_3 films were mostly reported only for RT grown samples (Haque et al., 2018), whereas the crystallization of amorphous Sb_2Se_3 thin films was reported by annealing at 448 K under vacuum and at 423 K in air (Abdel-Salam and Abdel-Wahabb, 1992). These results support our prediction that amorphous structure is mainly affected by low hydrogen flow. Although these films are almost amorphous, they exhibited small (2 2 1) peaks. Chen and co-authors reported that [2 2 1] orientation was found to be beneficial to for PV performance, as $(\text{Sb}_4\text{Se}_6)_n$ ribbons align perpendicular to the substrate surface (Chen et al., 2017a; Zhou et al., 2015). Hence, their Sb_2Se_3 films with [2 2 1] orientation yielded the highest free charge carrier mobility and the highest performance compared to those with other orientation, e.g. [1 2 0] (Chen et al., 2017b). With increasing the flow rate of the transport gas, e.g. (18–20) cm^3/min at T_s of (770–790) K, thin films grown with polycrystalline structure. Presumably, crystallization of Sb_2Se_3 thin films was affected by high flow rate of hydrogen. Despite the disappearance of the (2 2 1) peak, these films exhibited several peaks of orthorhombic Sb_2Se_3 , including the (2 1 1) peak (see Fig. 1). Tang and co-workers reported that Sb_2Se_3 grains with [2 1 1] orientation could also positively contribute for enhancement of the PV performance due to the nearly perpendicular alignment of the $(\text{Sb}_4\text{Se}_6)_n$ ribbons (with slightly tilted angle) to the substrate surface (Zhou et al., 2015).

Fig. 2 shows the SEM images of Sb_2Se_3 thin films grown in low (5–7) cm^3/min and high (18–20) cm^3/min hydrogen flow rates at different substrate temperatures. As-shown, films grown in low hydrogen flow rate exhibit smooth surface with small crystal grains on it (see Fig. 2a, b). This supports aforementioned discussion on XRD results that these films are almost amorphous with small (2 2 1) peaks. Apparently, Sb_2Se_3 crystals are not large enough to form polycrystalline structure, yet these films depicted [2 2 1] orientation (cf. Fig. 1). This may be due to the lack of gas flow to carry molecules towards the substrate. On the other hand, films grown in high hydrogen flow rate exhibited larger grains compared to those films grown in low hydrogen flow rate (Fig. 2c, d). It is likely that the flow rate is adequate to make optimal growth condition to grow Sb_2Se_3 crystals on the substrate, which confirms the above-mentioned XRD results that the films have polycrystalline structure. Although these films are polycrystalline, their surface morphology is dissimilar. Here not only the influence of the flow rate of the transport gas, but also effect of the substrate temperature has to be considered, since polycrystalline film grown at 770 K exhibit smoother surface in comparison to the sample grown at 790 K. Re-evaporation of Se is expected at higher substrate temperatures, which will be discussed below. EDX measurements revealed that low (high) hydrogen flow rate yielded Se enriched (Sb enriched) Sb_2Se_3 thin films, e.g. Sb/Se ratios of about 0.24 and 1.54 were depicted for the films grown in the hydrogen flow rates of 7 cm^3/min and 20 cm^3/min , respectively (see Fig. 3). Low hydrogen flow rate was not sufficient to carry out enough Sb-Se atoms to make Sb_2Se_3 thin films with stoichiometric composition, hence Se-rich condition could be the reason for the film growth with amorphous nature with smooth surface. Appearance of (2 2 1) peak in this film can be explained with chemical bond approach (Shaaban et al., 2007) as follows: different kinds of atoms (Sb-Se) combine more favourably in comparison to the same kind (Sb-Sb or Se-Se). This might be the reason for the appearance of [2 2 1] orientation in Sb_2Se_3 films grown in the low hydrogen flow rate although these films had low Sb content. With increasing hydrogen flow rate, the samples grown with higher Sb content (see Fig. 3b), where the probability of Sb-Se bonds increases in Sb_2Se_3 film. Consequently, Sb_2Se_3 film tends to grow with polycrystalline structure, which is apparent from XRD data and SEM images. This supports our prediction that optimized hydrogen flow rate is needed to grow Sb_2Se_3 thin films with

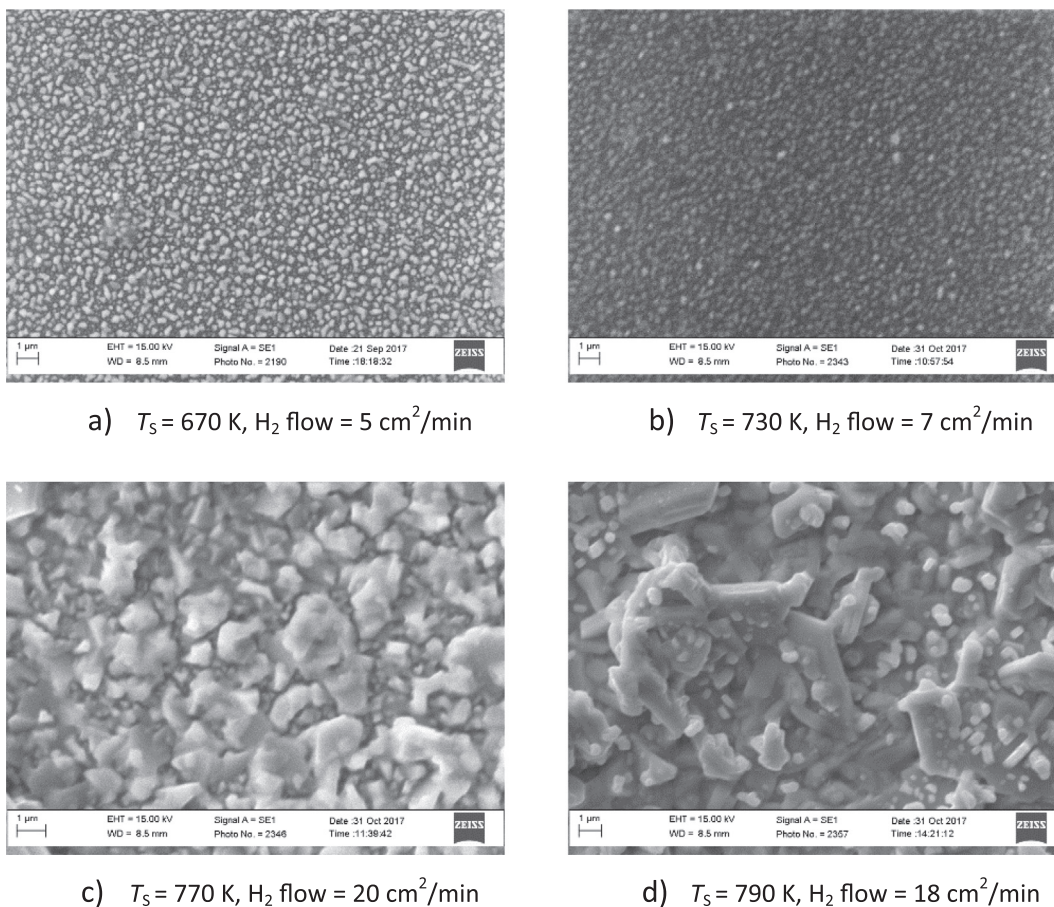


Fig. 2. SEM images of Sb_2Se_3 thin films grown in (a, b) low hydrogen flow rate of (5–7) cm^2/min and (c, d) high hydrogen flow rate of (18–20) cm^2/min at indicated substrate temperatures. The images were recorded at an acceleration voltage of 15 kV with a working distance of 8.5 mm.

desired chemical composition. Deficiency of Se in Sb_2Se_3 film at high substrate temperature could be due to the re-evaporation of Se. Salomé and co-authors also observed the similar effect of the Se deficiency during the deposition of $Cu_2ZnSnSe_4$ films at substrate temperature of 720 K (Salomé et al., 2010). In order to minimize the Se loss by re-evaporation from the sample, they turned off the substrate heater and allowed the substrate to cool down naturally at the end of the deposition process, while Se source (528 K) was turned off only when the substrate temperature reached 543 K. Se vacancy was argued to increase the density of recombination centres both inside and at the surface of Sb_2Se_3 (Li et al., 2016), which would lead low device performance via poor spectral response. Since post selenization step

compensated the Se vacancy and enhanced the device performance (Leng et al., 2016), additional selenization step is also believed to be beneficial for our samples grown at high substrate temperatures.

Transmission measurements revealed that optical bandgap and absorption coefficient of polycrystalline films are ~ 1.1 eV and $\sim 10^5 cm^{-1}$, respectively. This value of the optical bandgap is in agreement with literature values, where Chen and co-authors reported that polycrystalline Sb_2Se_3 film was an intrinsically indirect bandgap ($E_{g,i}$) material with the lowest $E_{g,i}$ of 1.03 ± 0.01 eV and the lowest direct bandgap of $E_{g,d} \approx 1.17 \pm 0.02$ eV at 300 K (Chen et al., 2015). As summarized in Table 1, obtained polycrystalline Sb_2Se_3 films have p -type conductivity with dark electrical conductivity of $\sim 10^{-7} (\Omega cm)^{-1}$

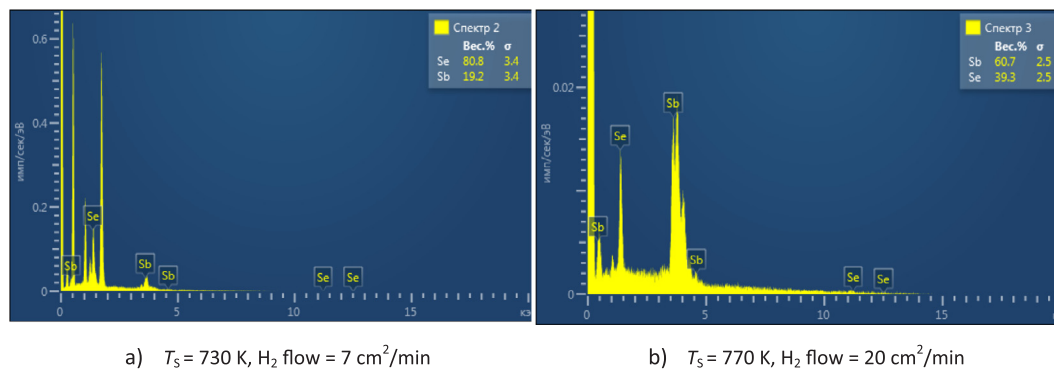


Fig. 3. Results of energy dispersive X-ray spectroscopy analysis for Sb_2Se_3 thin films grown at indicated substrate temperatures in (a) low hydrogen flow rate of $7 cm^2/min$ which yielded Se-rich film with Sb = 19.2 wt%, Se = 80.8 wt% and (b) high hydrogen flow rate of $20 cm^2/min$ which exhibited Sb-rich film with Sb = 60.7 wt%, Se = 39.3 wt%.

Table 1
Electrical and optical properties of polycrystalline Sb₂Se₃ thin film grown in hydrogen flow rate of 20 cm²/min.

Material	Evaporator temperature, (K)	Substrate temperature, (K)	Grain size, (μm)	Thickness, (μm)	Type of conductivity	Conductivity, (Ω cm) ⁻¹	Absorption coefficient, (cm ⁻¹)	Bandgap, (eV)
Sb ₂ Se ₃	900	770	1–2	~2	p	1.7 × 10 ⁻⁷	10 ⁵	1.1

which was similar to literature values, where Rodriguez-Lazcano et al. reported that Sb₂Se₃ thin films are photosensitive, with dark and photoconductivity values are 2 × 10⁻⁸ and 10⁻⁶ (Ω cm)⁻¹, respectively (Rodríguez-Lazcano et al., 2005).

4. Conclusions

Fabrication of Sb₂Se₃ thin films the first time by non vacuum chemical molecular beam deposition (CMBD) method has been reported. The morphological and structural properties of the films were studied as a function of the hydrogen flow rate at different substrate temperature. Experimental data showed that low hydrogen flow resulted to grow Se-rich Sb₂Se₃ films and the samples have almost amorphous structure, yet exhibited small (2 2 1) peaks. In contrast, in higher hydrogen flow rate, the films have Sb-rich composition and polycrystalline structure, which exhibited (2 1 1) peaks. Sb enrichment is correlated with high substrate temperature which increases the re-evaporation of Se from the film. Electrical and optical measurements revealed that polycrystalline Sb₂Se₃ films show p-type conductivity and optical bandgap value of about 1.1 eV with high absorption coefficient of 10⁵ cm⁻¹. These experimental results showed that CMBD grown films can be used as absorber layer for fabrication of thin film solar cells.

Acknowledgement

This work was supported by Fundamental Grant of Uzbekistan Academy of Sciences (No. FA-F3-003) and Junior Research Fund (No. YoFA-Atech-2018-205).

References

Abdel-Salam, F., Abdel-Wahabb, E., 1992. Structural variations in antimony selenide. *Vacuum* 43, 849–853.

Bajpeyee, A.U., 2012. Deposition and characterization of antimony selenide thin films. *Multilogic Sci. Int. Refreed Indexed Quart. J.* 2 (2), 38–43.

Chantana, J., Suzuki, K., Minemoto, T., 2017. Introduction of Na into Cu₂ZnSnS₄ thin film for improvement of its photovoltaic performances. *Sol. Energy Mater. Sol. Cells* 168, 207–213.

Chen, C., Li, W., Zhou, Y., Chen, C., Luo, M., Liu, X., Zeng, K., Yang, B., Zhang, C., Han, J., Tang, J., 2015. Optical properties of amorphous and polycrystalline Sb₂Se₃ thin films prepared by thermal evaporation. *Appl. Phys. Lett.* 107, 043905.

Chen, C., Wang, L., Gao, L., Nam, D., Li, D., Li, K., Zhao, Y., Ge, C., Cheong, H., Liu, H., Song, H., Tang, J., 2017a. 6.5% Certified SbSe solar cells using PbS colloidal quantum dot film as hole transporting layer. *ACS Energy Lett.* 2, 2125–2132.

Chen, C., Bobela, D., Yang, Y., Lu, S., Zeng, K., Ge, C., Yang, B., Gao, L., Zhao, Y., Beard, M.C., Tang, J., 2017b. Characterization of basic physical properties of Sb₂Se₃ and its relevance for photovoltaics. *Front. Optoelectron.* 10, 18–30.

Choi, Y.C., Mandal, T.N., Yang, W.S., Lee, Y.H., Im, S.H., Noh, J.H., Seok, S.I., 2014. Sb₂Se₃-sensitized inorganic-organic heterojunction solar cells fabricated using a single-source precursor. *Angew. Chem. Int. Ed.* 53, 1329–1333.

Green, M., Yoshihiro, H., Duplon, E.D., Levi, D.H., Hohl-Ebinger, J., Ho-Baillie, A.W.Y., 2017. Solar cell efficiency tables (version 51). *Progr. Photovolt.: Res. Appl.* 26, 3–12.

Guha, S., 2017. Thin-film photovoltaics: Buffer against degradation. *Nat. Energy* 2, 17057.

Hartnauer, S., Körbel, S., Marques, M.A.L., Botti, S., Pistor, P., Scheer, R., 2016. Research update: stable single-phase Zn-rich Cu₂ZnSnSe₄ through in doping. *APL Mater.* 4, 070701.

Haque, F., Elumalai, N.K., Wright, M., Mahmud, M.A., Wang, D., Upama, M.B., Xu, C., Uddin, A., 2018. Annealing induced microstructure engineering of antimony tri-selenide thin films. *Mater. Res. Bull.* 99, 232–238.

Jackson, P., Wuerz, R., Hariskos, D., Lotter, E., Witte, W., Powalla, M., 2016. Effects of heavy alkali elements in Cu(In,Ga)S₂ solar cells with efficiencies up to 22.6%. *Phys. Status Solidi RRL* 10 (8), 583–586.

Khan, M.D., Aamir, M., Sohail, M., Sher, M., Akhtar, J., Malik, M.A., Revaprasadu, N., 2018. Novel single source precursor for synthesis of Sb₂Se₃ nanorods and deposition of thin films by AACVD: Photo-electrochemical study for water reduction catalysis. *Sol. Energy* 169, 526–534.

Kulkarni, A., Arote, S., Pathan, H., Patil, R., 2015. Sb₂Se₃ sensitized heterojunction solar cells. *Mater. Renew. Sustain. Energy* 4, 1–6.

Leng, M., Luo, M., Chen, C., Qin, S., Chen, J., Zhong, J., Tang, J., 2014. Selenization of Sb₂Se₃ absorber layer: an efficient step to improve device performance of CdS/Sb₂Se₃ solar cells. *Appl. Phys. Lett.* 105, 083905.

Li, K., Kondrotas, R., Chen, C., Lu, S., Wen, X., Li, D., Luo, J., Zhao, Y., Tang, J., 2018. Improved efficiency by insertion of Zn_{1-x}Mg_xO through sol-gel method in ZnO/Sb₂Se₃ solar cell. *Sol. Energy* 167, 10–17.

Li, Z., Zhu, H., Guo, Y., Niu, X., Chen, X., Zhang, C., Zhang, W., Liang, X., Zhou, D., Chen, J., Mai, Y., 2016. Efficiency enhancement of Sb₂Se₃ thin-film solar cells by the co-evaporation of Se and Sb₂Se₃. *Appl. Phys. Express* 9, 052302.

Liu, X., Chen, J., Luo, M., Leng, M., Xia, Z., Zhou, Y., Qin, S., Xue, D.J., Lv, L., Huang, H., Niu, D., Tang, J., 2014. Thermal evaporation and characterization of Sb₂Se₃ thin film for substrate Sb₂Se₃/CdS solar cells. *ACS Appl. Mater. Interfaces* 6, 10687–10695.

Polman, A., Knight, M., Garnett, E.C., Ehrler, B., Sinke, W.C., 2016. Photovoltaic materials: present efficiencies and future challenges. *Science* 352, aad4424.

Razykov, T.M., 1991. Chemical molecular beam deposition of II-VI binary and ternary compound films in gas flow. *Appl. Surf. Sci.* 48/49(1), 89–92.

Razykov, T.M., Shukurov, A.X., Atabayev, O.K., Kuchkarov, K.M., Boltaev, G.S., Kutlimurotov, B.R., Mavlonov, A.A., 2017. Characterization of Sb₂Se₃ thin films fabricated by CVD. *Geliotechnika* 3, 7–11.

Razykov, T.M., Boltaev, G.S., Bosio, A., Ergashev, B., Kouchkarov, K.M., Mamarsulov, N.K., Mavlonov, A.A., Romeo, A., Romeo, N., Tursunkulov, O.M., Yuldoshov, R., 2018. Characterisation of SnSe thin films fabricated by chemical molecular beam deposition for use in thin film solar cells. *Sol. Energy* 159, 834–840.

Ren, Y., Scragg, J.J., Ericson, T., Kubart, T., Platzer-Björkman, C., 2015. Reactively sputtered films in the Cu₂-ZnS-SnS₂ system: From metastability to equilibrium. *Thin Solid Films* 582, 208–214.

Rodríguez-Lazcano, Y., Pena, Y., Nair, M.T.S., Nair, P.K., 2005. Polycrystalline thin films of antimony selenide via chemical bath deposition and post deposition treatments. *Thin Solid Films* 493, 77–82.

Salomé, P.M.P., Fernandes, P.A., da Cunha, A.F., 2010. Influence of selenization pressure on the growth of Cu₂ZnSnSe₄ films stacked metallic layers. *Phys. Status Solidi C* 7, 913–916.

Shaaban, E., Abdel-Rahman, M., Yousef, E., Dessouky, M., 2007. Compositional dependence of the optical properties of amorphous antimony selenide thin films using transmission measurements. *Thin Solid Films* 515, 3810–3815.

Siol, S., Schulz, P., Young, M., Borup, K.A., Teeter, G., Zakutayev, A., 2016. Combinatorial in situ photoelectron spectroscopy investigation of Sb₂Se₃/ZnS heterointerfaces. *Adv. Mater. Interfaces* 3, 1600755.

Sun, P., Wu, Z., Ai, C., Zhang, M., Zhang, X., Huang, N., Sun, Y., Sun, X., 2016. Thermal evaporation of Sb₂Se₃ as novel counter electrode for dye-sensitized solar cells. *Chem. Select* 1, 1824–1831.

Tiwari, K.J., Ren, M.Q., Vajandar, S.K., Osipowicz, T., Subrahmanyam, A., Malar, P., 2018. Mechanochemical bulk synthesis and e-beam growth of thin films of Sb₂Se₃ photovoltaic absorber. *Sol. Energy* 160, 56–63.

Wen, X., Chen, C., Lu, S., Li, K., Kondrotas, R., Zhao, Y., Chen, W., Gao, L., Wang, C., Zhang, J., Niu, G., Tang, J., 2018. Vapor transport deposition of antimony selenide thin film solar cells with 7.6% efficiency. *Nature Communications* 9, 2179.

Whittles, T.J., Veal, T.D., Savory, C.N., Welch, A.W., de Souza Lucas, F.W., Gibbon, J.T., Birkett, M., Potter, R.J., Scanlon, D.O., Zakutayev, A., Dhanak, V.R., 2017. Core levels, band alignments, and valence-band states in CuSbS₂ for solar cell applications. *ACS Appl. Mater. Interfaces* 9, 41916–41926.

Yoshikawa, K., Kawasaki, H., Yoshida, W., Irie, T., Konishi, K., Nakano, K., Uto, T., Adachi, D., Kanematsu, M., Uzu, H., Yamamoto, K., 2017. Silicon heterojunction solar cell with interdigitated back contacts for a photoconversion efficiency over 26%. *Nat. Energy* 2, 1–8.

Yuan, C., Zhang, L., Liu, W., Zhu, C., 2016. Rapid thermal process to fabricate Sb₂Se₃ thin film for solar cell application. *Sol. Energy* 137, 256–260.

Zakutayev, A., 2017. Brief review of emerging photovoltaic absorber materials. *Curr. Opin. Green Sustain. Chem.* 4, 8–15.

Zhou, Y., Leng, M., Xia, Z., Zhong, J., Song, H., Liu, X., Yang, B., Zhang, J., Chen, J., Zhou, K., Han, J., Cheng, Y., Tang, J., 2014. Solution-processed antimony selenide heterojunction solar cells. *Adv. Energy Mater.* 4, 1301846.

Zhou, Y., Wang, L., Chen, S., Qin, S., Liu, X., Chen, J., Xue, D.-J., Luo, M., Cao, Y., Cheng, Y., 2015. Thin-film Sb₂Se₃ photovoltaics with oriented one-dimensional ribbons and benign grain boundaries. *Nat. Photon.* 9, 1–8.